

## Finite element method based design and performance analysis of universal motor for agro applications

Sudhir Kumar Sharma, Manpreet Singh Manna

Department of Electrical and Instrumentation Engineering, Sant Longowal Institute of Engineering and Technology, Punjab, India

---

### Article Info

#### Article history:

Received Jun 4, 2022

Revised Sep 29, 2022

Accepted Oct 19, 2022

---

#### Keywords:

Ansys maxwell

Brush angle

Pole embrace factor

Steel material

Universal motor

---

### ABSTRACT

A universal motor is one that is capable of operating on either AC or DC power supply. The commutator is a component of the motor that has a significant impact on how efficiently the motor operates. It is essential to conduct an analysis of the pole structure of the universal motor in order to investigate the many aspects. The parametric study of a universal motor with a rating of 1 horsepower and 15,000 revolutions per minute that was designed with various combinations of brush angle and pole embrace factor for use in agricultural applications. The purpose of this study is to improve the effectiveness of the motor while preserving the ideal tolerance range for the model's other parameters as much as possible. The approach now allows for a greater degree of personalization for each distinct combination of factors. With the assistance of the finite element method (FEM), the transient solution is carried out so that the performance of the motor can be evaluated more accurately. The model that has been designed provides major design improvements, one of which is an improved average torque.

*This is an open access article under the [CC BY-SA](https://creativecommons.org/licenses/by-sa/4.0/) license.*



---

### Corresponding Author:

Sudhir Kumar Sharma

Department of Electrical and Instrumentation Engineering

Sant Longowal Institute of Engineering and Technology

SLIET Longowal, SLIET Rd, Punjab 148106, India

Email: sudhirs390@gmail.com

---

## 1. INTRODUCTION

Electrical machines play an essential part in industries that deal with energy conversion. These machines can be used for many purposes like industrial and agro applications. There are some conventional motors present in the market that has proven their worth, like single phase induction motor, permanent magnet DC (PMDC) motor, brushless DC (BLDC) motor and universal motor [1]. The universal motors can be used in many domestic applications such as mixers, grinders, vacuum cleaners; small power tools, some industrial products, in ac drive circuits, and agriculture applications [2]. Universal motors have a high starting torque and a variable speed characteristic. The motor has worked on high-speed rotation, low cost, good power density, reliable, controllable and use simple materials. Due to the presence of brushes on the commutator, it faces wear and tear mechanism, which leads to less efficiency than DC motor [3], [4]. The design of electric machine is a tedious task; it consumes a lot of time and effort. It is good practice to design a motor before building it as it saves time and money [5].

In recent years many researchers have done their practices to enhance the performance of universal motor present in the literature. The author economically designed motor for feasible applications using rotor ends by changing the magnetic flux density and material, to determine eddy current and loss analysis, there is enhancement in performance [6]-[9]. The author compared the performance of universal motor and BLDC motor drive using simulink for the grinder and mixer [10]. The author presented the behavior scanning of the

universal motor works on the AC and DC supply, which was achieved with MATLAB Simulink's help to know the motor's better performance on which supply results that motor performs better on DC supply [11]. The author analysed the core losses of the induction motor for the various steel materials [12]. The author design motor for fan application with characteristic of torque ripple reduction and improved magnetic behaviour [13], [14]. The predictive approach was applied to control the tracking problem for polysolenoid motor [15]. Design motor with the even number of pole/slot combination for static and dynamic analysis [16]. Proposed 550-watt deep slot universal motor run on 9,500 rpm speed for powerful electric tools. The motor was simulated on finite element method (FEM) based MagNet software and experimentally tested. The analysis was performed with different variables to enhance the performance of the respective motor [17]. Innovatively proposed a combination of two windings in the existing design of the universal motor, which significantly improves the motor's torque ripples and core losses [18]. Efficiency and loss analysis of the universal motor by extracting mathematical modeling. The power loss of the motor universal was improved with the help of MATLAB Simulink software for mixer grinder applications [19]. A performance comparison of 2 poles and 4 poles universal motor, and the results were given at the rated speed of the motor. It was stated that the commutation process of a 4-pole motor is better than a 2-pole motor which provided a better new design of universal motor by varying the numeral of armature slots and simultaneously [20]. A comparison of induction motor and universal motor model for the washing machine application. The performance parameters efficiency, induced voltage, current, speed and torque was determined and compared with the experimental setup [21]. The universal motor design for the washer application. The model was simulated in Simulink of MATLAB based on the AC and DC supply the difference between the results of transformer voltage, commutation, saturation effects, and armature reaction were compared and analysed experimentally [22]. Lin *et al.* [23] proposed the model of a universal motor to improve the commutation process by shifting the brush angle from the neutral position by just not concentrating on the d-axis and q-axis with finite element analysis. Miller and Willing [24] were willing to analytically calculate all the values of inductances for the motor design by shifting the lag coil angle. Then, the designed model was analysed with finite element analysis (FEA) and experimentally. The commutation phenomenon of universal motor considering the optimum values of fraction of commutator width and brush width using FLUX<sup>R</sup> software. The effect of this process on the efficiency and brush life was examined [25]. The universal motor to determine brush to bar voltage drop through FEA having time stepping analysis. The design was observed compared with conventional analysis was more accurate [26]. The universal motor model to determine the self-inductance and mutual inductance coefficients, as well as the electromotive force created in the coil sections taking into account magnetic saturation, the brush-commutator voltage drop, and electric arc was determined [27].

The objective of the present work is to show that the change in pole embrace factor and brush angle have considerable effects on the performance of universal motor with the help of parametric analysis. The finite element method-based software helps to realize the performance of the motor. The electrical and transient analysis of the solution determined the better average torque and efficiency of the motor. The universal motor is studied for specific agro applications like grinding, winnowing, and threshing.

## 2. METHOD

The universal motor mathematical model based on mathematical equations of voltage and power is presented in this section. Figure 1, shown is the universal motor equivalent circuit. The operating conditions of this motor voltage and current equations are the same as a DC series motor.

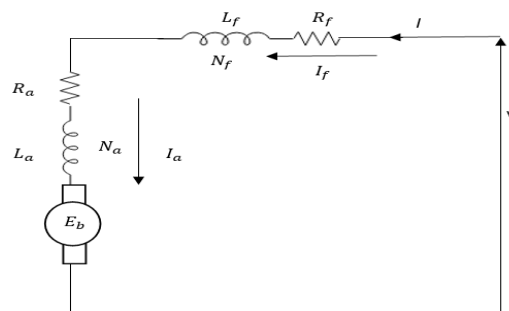


Figure 1. Equivalent circuit of universal motor

The supply current is equal to the armature current, and field currents is mentioned in (1). Voltage drops across field winding, back emf, voltage drops across armature winding, mutual inductance voltage drops, and the voltage drop across brushes are calculated according to (2)-(6) respectively.

$$I = I_a = I_f \quad (1)$$

$$V_f = R_f I_f + L_f \left( \frac{dI_f}{dt} \right) \quad (2)$$

$$E_b = \frac{\phi Z N P}{60 A} \quad (3)$$

$$V_a = R_a I_a + L_a \left( \frac{dI_a}{dt} \right) \quad (4)$$

$$E_m = L_a \left( \frac{dI}{dt} \right) dt \quad (5)$$

$$V = V_a + V_f + E_m + E_b + V_{bd} \quad (6)$$

Where,  $V$ =supply voltage,  $I$ =load current,  $E_b$ =back emf,  $V_{bd}$ =voltage drop across brushes,  $I_a$ =current of armature,  $I_f$ =field winding current,  $R_a$ =resistance of armature winding,  $R_f$ =resistance of field winding,  $L_a$ =inductance of armature winding,  $L_f$ =inductance of field winding,  $L_{af}$ =mutual inductance between armature winding and field,  $N_f$ =field winding number of rotational turns,  $N_a$ =number of turns of armature winding.

The thickness of brushes has a profound influence on the computation conditions. Total brush contact area per spindle is the ratio of current carried by each brush spindle to the current density in the brushes. The losses in the commutation processes are the brush contact losses and brush friction losses. The brush contact drop is independent of load current. The typical value of brush drop is around 1 volt. The brush friction loss depends upon the brush pressure, the commutator's peripheral speed and the friction coefficient between the brush and the commutator. It can be calculated as (7).

$$\text{Brush friction loss} = \mu P_b A_b V_c \quad (7)$$

Where  $\mu$ =coefficient of friction,  $P_b$ =brush contact pressure on commutator ( $N/m^2$ ),  $A_b$ =total contact area of all brushes, and  $V_c$ =peripheral speed of the commutator (m/s)

To avoid delayed commutation process, a heavy short circuit and spark at the brushes should be shifted backwards opposite to the direction of rotation for motors to bring them into the magnetic neutral zone. The effect of this brush shift is to resolve the armature winding into two component windings. The Winding produces some extra mmf, which acts directly against the field mmf. The armature winding produces cross magnetizing mmf whose axis is at  $90^\circ$  with respect to the main field; therefore, demagnetizing mmf is called the cross-magnetizing component of armature reaction.

$$\text{Demagnetizing mmf per pole} = \text{Total armature mmf} \left( \frac{2\alpha}{180} \right)$$

The cross magnetizing mmf per pole equals the difference between the total armature mmf per pole and the demagnetizing mmf per pole.

$$\text{Cross-magnetizing mmf per pole} = \text{Total armature mmf} \left( 1 - \frac{2\alpha}{180} \right)$$

## 2.1. Power losses in universal motor

Efficiency is the proportional ratio of output power to input power, which depends on various power losses, i.e., copper loss, brush loss, friction loss, core loss, and ventilation loss. The friction loss, brush loss, and ventilation loss depend on the motor speed.

### 2.1.1. Copper losses

Copper losses occur when current flows through a copper-made conductor, the copper loss is two types field winding copper loss and armature winding copper loss.

$$\text{Copper loss of field winding} = I_f^2 R_f$$

Copper loss of armature winding =  $I_a^2 R_a$

### 2.1.2. Core losses

Core losses occur in a magnet's core because of alternating magnetization, and core loss is the integral sum of eddy current and loss hysteresis loss. Hysteresis loss can be calculated by (8) and (9).

$$P_h = K_h B n f m \quad (8)$$

$$P_h = K_h \left(\frac{\phi}{4A}\right) n \left(\frac{PN}{2}\right) m \quad (9)$$

Where  $k_h$  is the material hysteresis constant,  $B$  is the flux density maximum,  $n$  is the exponent of material-dependent,  $f$  is the frequency,  $m$  is the mass,  $A$  area of core,  $P$  is number of poles,  $N$  is speed, and  $\phi$  is flux around the air gap. The eddy-current loss can be determined by (10) and (11).

$$P_e = K_e B^2 f^2 m \quad (10)$$

$$P_e = K_e \left(\frac{\phi}{4A}\right)^2 \left(\frac{PN}{2}\right)^2 m \quad (11)$$

Where  $k_e$  is the material-dependent constant of eddy current.

The frequency squared influences the eddy current loss and hysteresis loss, which rises linearly with frequency [28]. The representation of the pole embrace factor is given in Figure 2, which is defines as the ratio of pole arc to pole pitch of the motor. According to the literature, this factor must be less than unity or between zeros to unity [29].

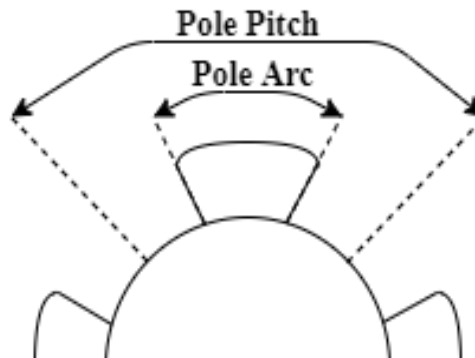


Figure 2. Representation of pole embrace factor

Previously, the researchers developed an equivalent circuit method to analyse the performance. But electromagnetic parameters were not appropriately analysed, which diverted the designing of the machine towards the use of advanced technologies of computational electromagnetics. Various computational methods are present to design electromagnetic device and electromechanical instruments. The finite element method is chosen among the various computational techniques to determine electromagnetic issues. It is the best method that the designer could assist, and the researcher can perform electromagnetic calculations on real-world problems [30]. The FEM is suitable for low-frequency electromagnetic problems, notably in rotating electrical machine design, among the several techniques available for handling electromagnetic difficulties. Finite element analysis is a computational tool that uses mesh generation techniques to divide a complex problem into small elements and software coded with a FEM algorithm. When using FEA, the complex problem is usually a physical system with the underlying physics expressed in either partial derivative equations (PDE) or integral equations. Simultaneously, finite element analysis tools could assist designers and researchers in performing electromagnetic calculations more accurately. In contrast, the divided small elements of the complex problem represent different areas in the physical system [5], [31]. Among the three main stages first one is pre-processing. This FEM tool involves various analysis of magnetostatic, steady state, thermal, eddy current, and transient of the non-linear, permanent magnet materials [32]. The application area widens in electromechanical, electrical instruments in which the discretization of the elements has been done on

geometrical domain. The intermediate stage includes the actual solution in which loading conditions has been applied and actual solution has been configured. The last stage is displaying the results through the graph or visual form, which is the post-processing stage [33], [34].

The design of a universal motor has been created using ANSYS Maxwell software. The power ratings of the motor considered are 1 hp and 120 V. The dimensional parameters of motor has been tabulated in the Table 1.

Table 1. Dimensional parameters of universal motor

Parameters	Values
Stator core outer Diameter ( $D_{so}$ )	61.7 mm
Rotor core outer Diameter ( $D_{ro}$ )	37 mm
Stack length	33.35 mm
Stator yoke thickness	5.2 mm
Rotor core Diameter ( $D_r$ )	12.1 mm
Frequency	50 Hz
Stator/rotor material	Steel_1008

Both stator and rotor core are made of steel\_1008. The magnetisation curve of the silicone material used is shown in the Figure 3. It has shown the magnetic field density transition value, i.e., 1.6 tesla. The material used has good thermal stability for the motor design having a 2/12 pole slot combination.

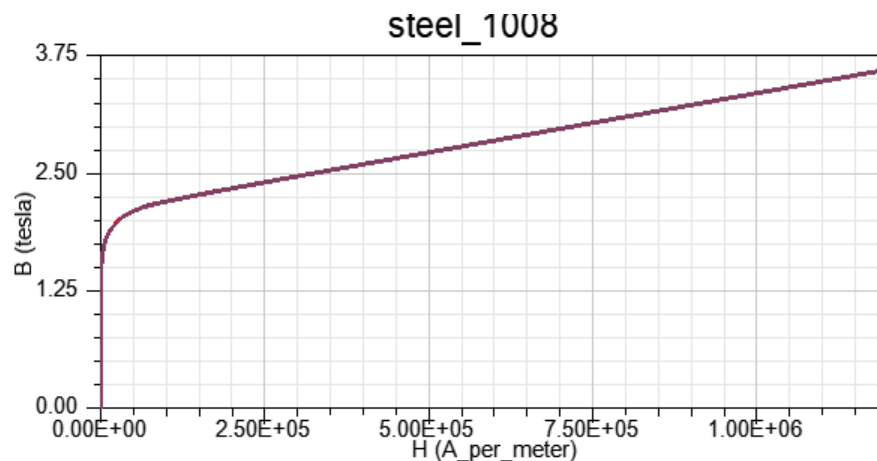


Figure 3. Magnetisation curve of steel\_1008 material

### 3. RESULTS AND DISCUSSION

The parametric approach method adopted for the performance analysis of the universal motor's model. The vital factors that should be considered are high efficiency, less loss, low volume and optimal cost. The efficiency parameter is determined to follow the model's requirement. The two variables selected are brush angle and pole embrace factor. There is a trade-off between the two variables w.r.t parameters. The value of the brush angle varies from  $5^\circ$  to  $22.5^\circ$  with the step value of  $2.5^\circ$ , and pole embrace value varies from 0.55 to 0.9 with the step value of 0.05 as a result of consideration of physical constraint. The parametric analysis has been performed to check the performance of the motor for total 64 values. Further, the optimization techniques are performed to analyse the results.

To select the optimum value of variables from the intermediate values for the rated torque, and the high efficiency performance criteria of the motor is followed. But it is not always easy to find the one single value. Sometimes better values lie in some region where one should decide taking into some priorities in the design. The graphical representation of rated torque with the variation of brush angle and pole embrace is shown in Figure 4. The graph depicts maximum value is 584.906 mNm at  $5^\circ$  and 0.85 pole embrace value and a minimum value 379.2 mNm at  $22.5^\circ$  and 0.9 value of pole embrace. Here the feasible region criteria is used for selection. The graphical representation of efficiency with variation of brush angle and pole embrace value is shown in Figure 5. The maximum efficiency of 73.15% lies at point  $5^\circ$  and 0.65 value and the minimum value of efficiency 51.273% lies at point  $5^\circ$  and 0.9 value of pole embrace factor.

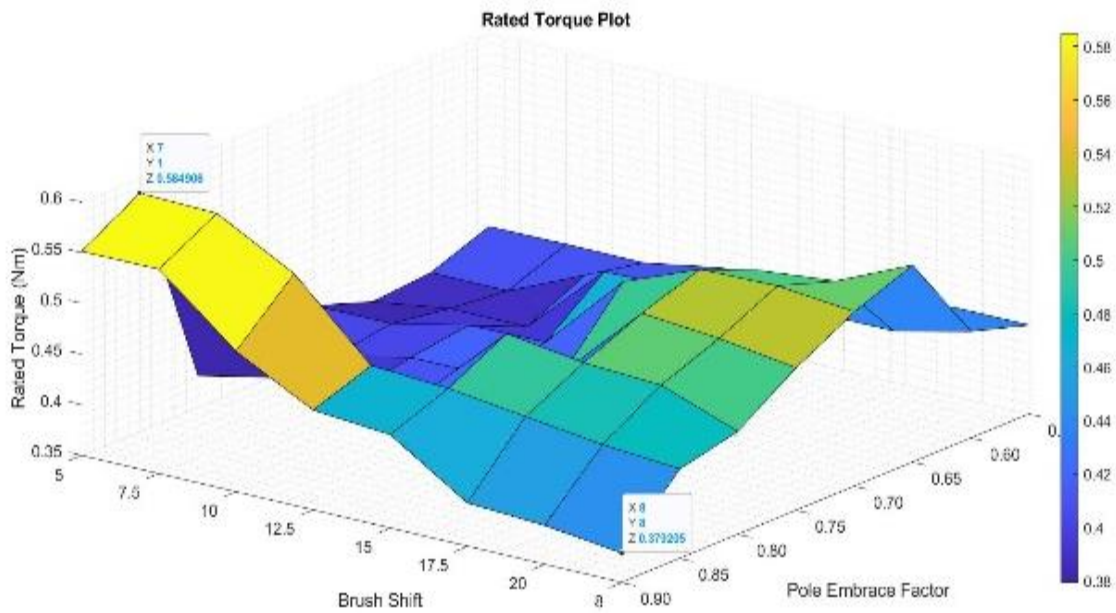


Figure 4. Rated torque w.r.t. pole embrace factor and brush angle

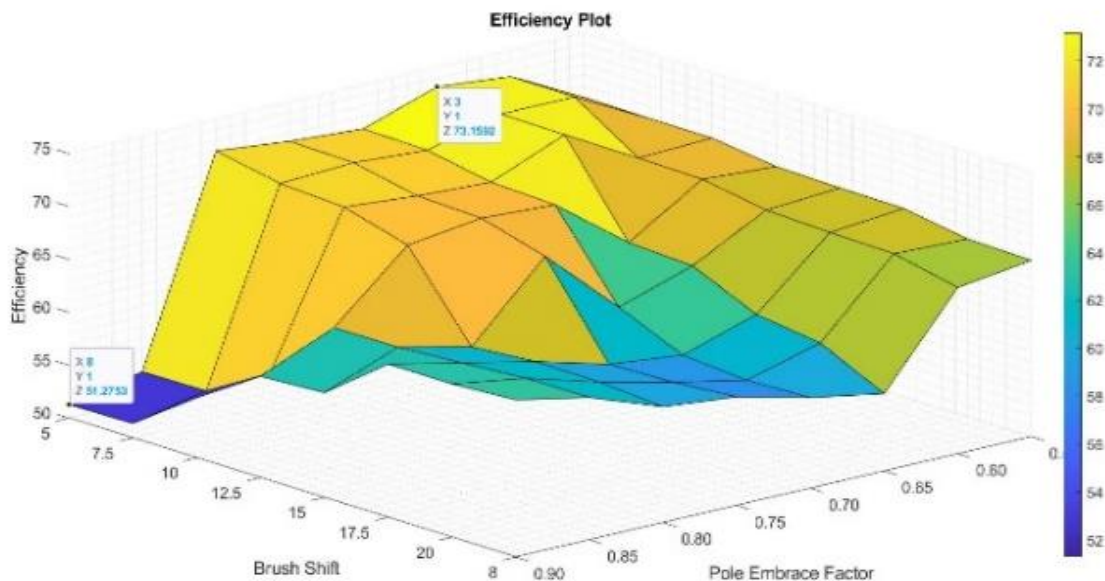


Figure 5. Efficiency w.r.t. pole embrace factor and brush angle

From the above results the optimum point is selected based on the high performance of the motor. It is shown that at 0.65 pole embrace and  $5^\circ$  brush angle, motor has high efficiency as compared to the other combination values. Moreover, for the rated torque, the intermediate value selected also lies at this point. Further analysis of the motor has been performed at the optimum value of 0.65 and  $5^\circ$  keeping rest of the dimensional parameters same. The graph of air gap flux density with variation of electric degree of rotor is shown in Figure 6. It depicts value of air gap flux density is maximum between 35 to 140 electrical degrees. The graph of output torque with variation of speed is shown in Figure 7 which depicts the starting output torque is 1.3 Nm with respect to variable speed of rotor and rated torque is 0.38 Nm with a rated speed.

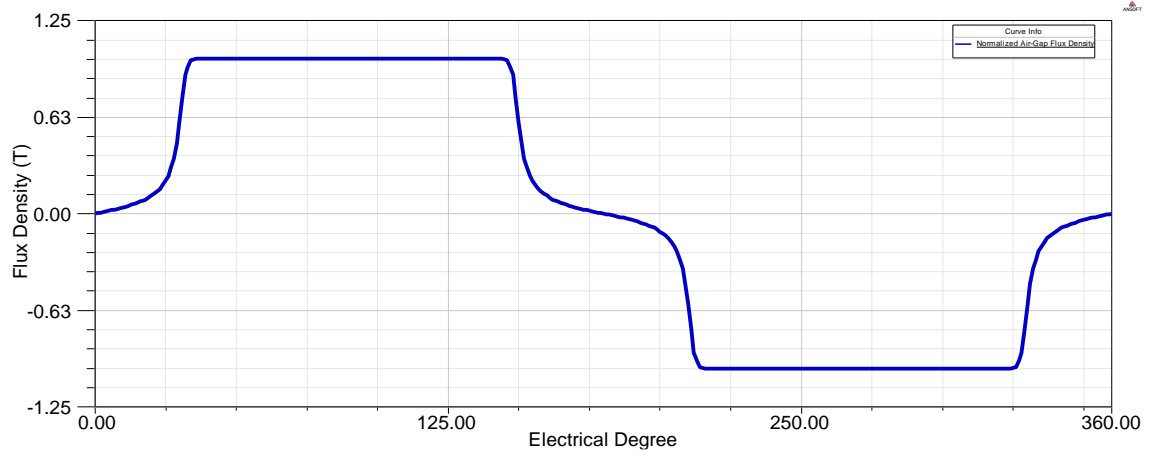


Figure 6. Air gap flux density w.r.t electrical degree curve

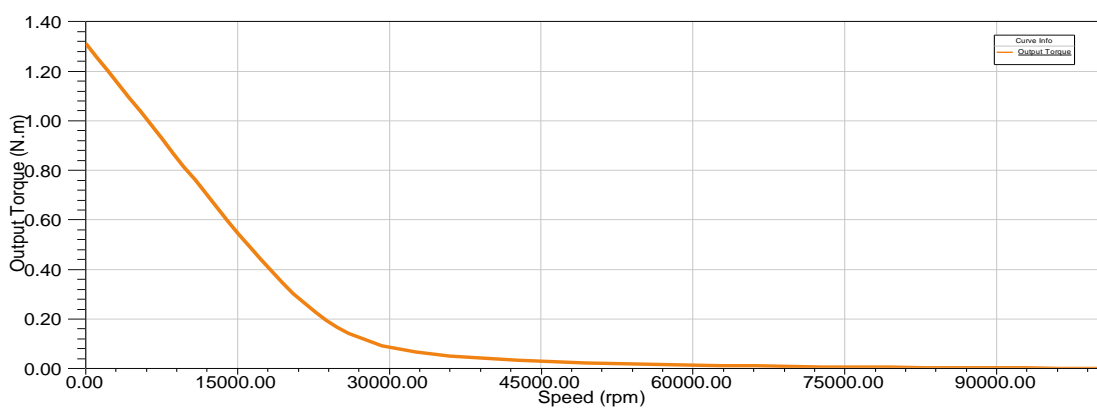


Figure 7. Output torque w.r.t speed curve

The graphical representation of efficiency with speed variation is shown in Figure 8. It depicts that at the optimum point of selection; for the rated speed of 15,000 rpm the value of efficiency is 63.1% and maximum efficiency is 86.11% when rotor at 29,321 rpm speed of the motor. The graphical representation of input current and speed is shown in Figure 9. This depicts the starting current motor takes is 15.2 A and rated current of motor is 4.92 A with variation of speed of the rotor.

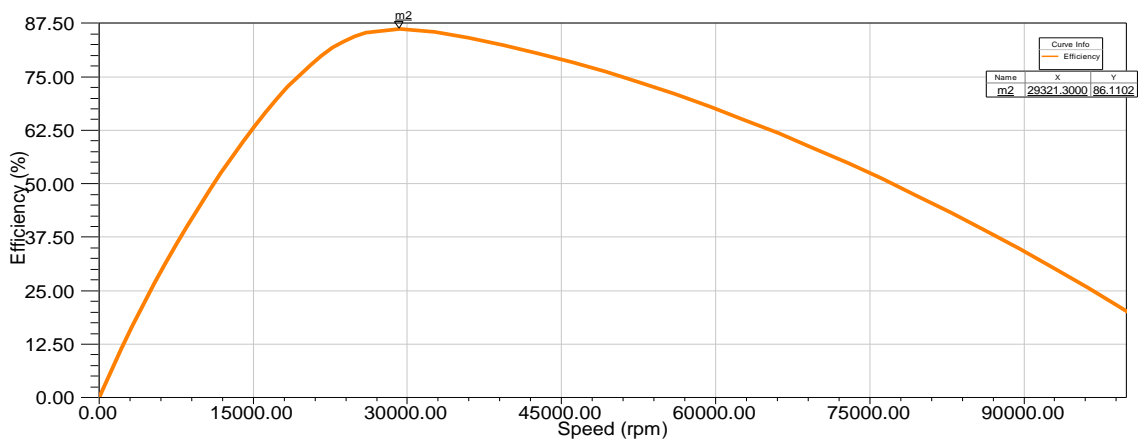


Figure 8. Efficiency w.r.t speed (rpm) curve



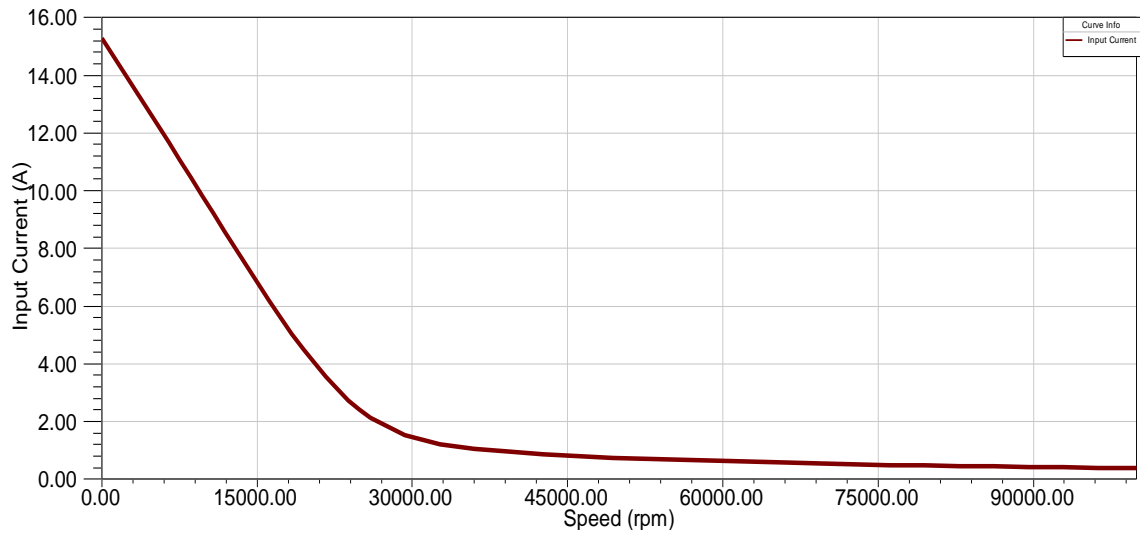


Figure 9. Input current w.r.t speed curve

The transient analyses of motor are carried out at the optimum point using the FEA, which has four steps. The initial step involves motor modelling in which the meshing formulation of the model is performed. In addition, the analysis is carried out using FEA Solver. Then, using the interpolation function, the solution for the entire mesh is approximated, and based on the solution, desired parameters or variables derived are computed in the whole domain. The overview of the FEM based analysis model of the motor is given in Figure 10. The motor with plot meshes of 4027 shown in Figure 11. It shows the mesh formation at a specific time and rotor position.

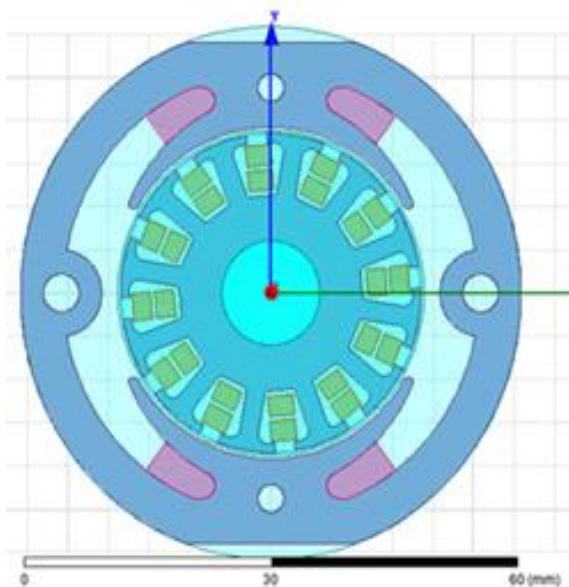


Figure 10. FEM analysis of motor

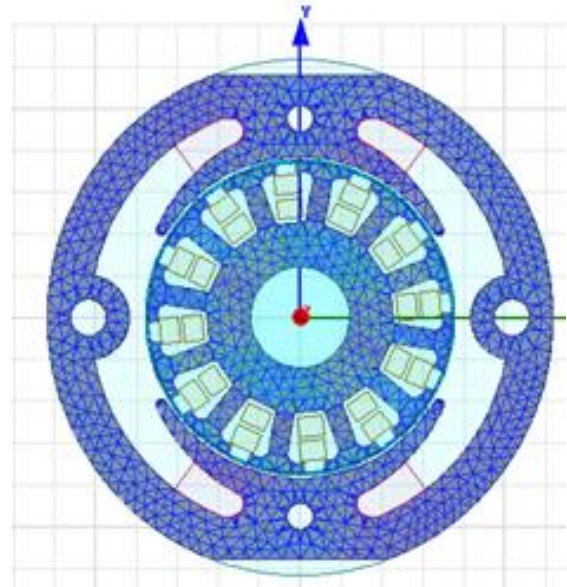


Figure 11. Plot mesh FEM analysis of motor

The electromagnetic torque of the motor with change of time is shown in Figure 12. The average torque value is 206 Nm, minimum torque is 390.5 Nm and the maximum value is 568.6 Nm. The torque ripple of the model is 0.864. The winding current for the coil 0 is shown in Figure 13.



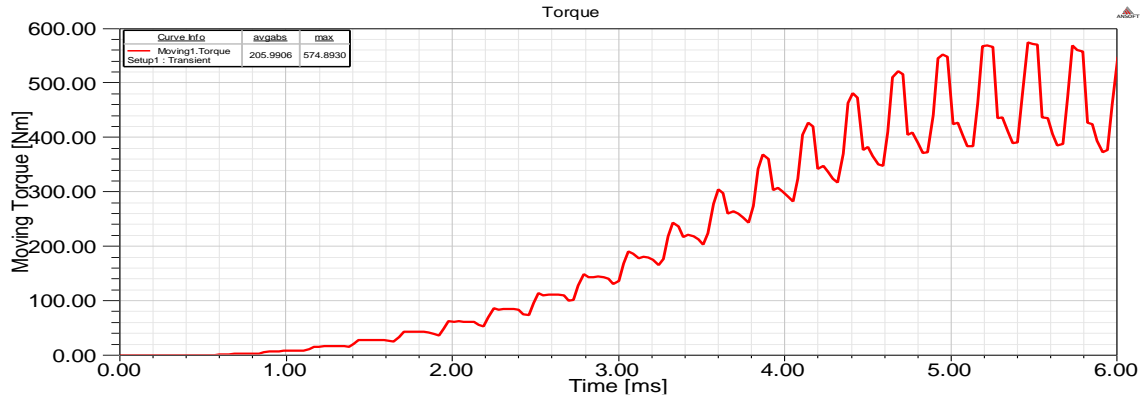


Figure 12. Electromagnetic torque with the change of time

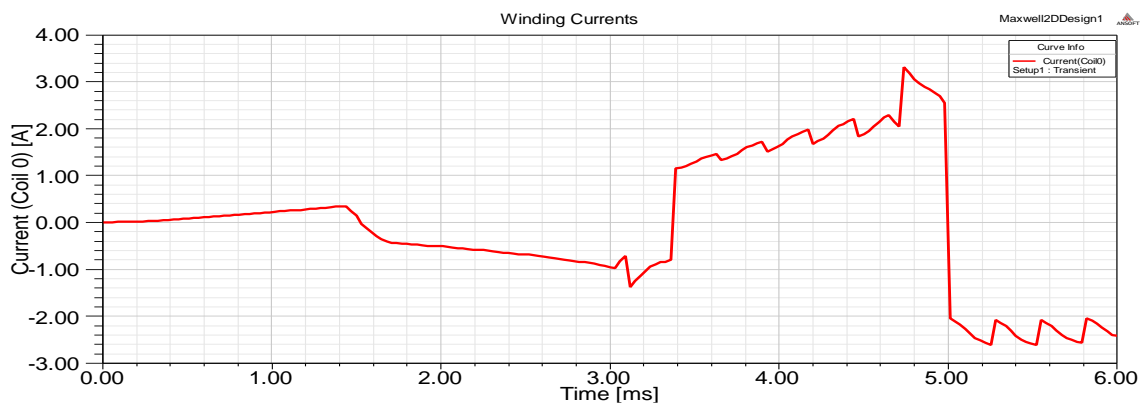


Figure 13. Winding current with the change of time

The magnetic field density and magnetic flux lines of specific rotor position is shown in Figure 14 and Figure 15, respectively. It shows that the motor does not operate at a value when the model runs into saturation condition. The magnetic flux lines are lies in between the boundary region of the model.

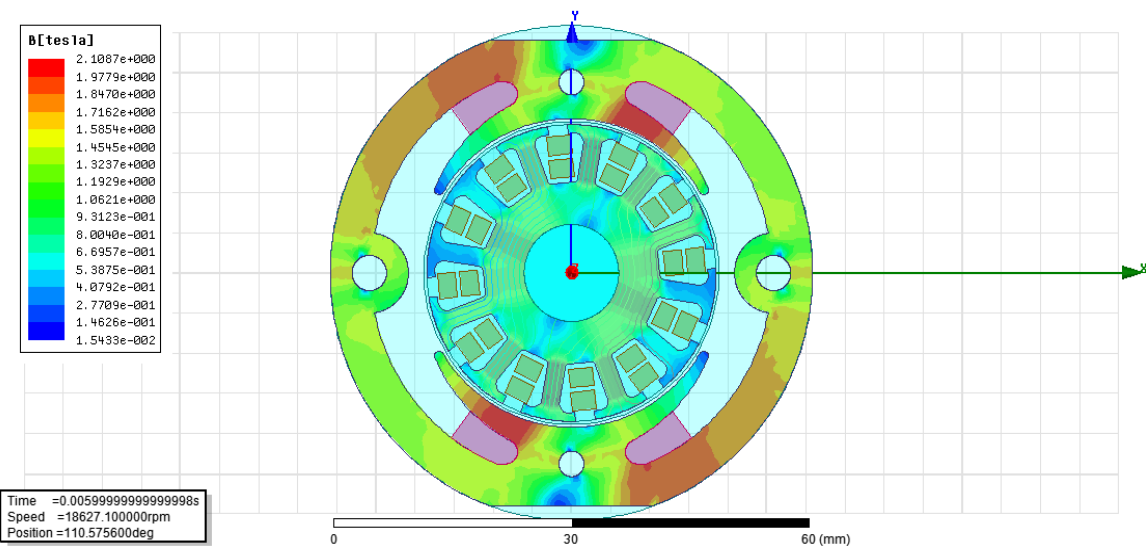


Figure 14. Magnetic flux density of the motor

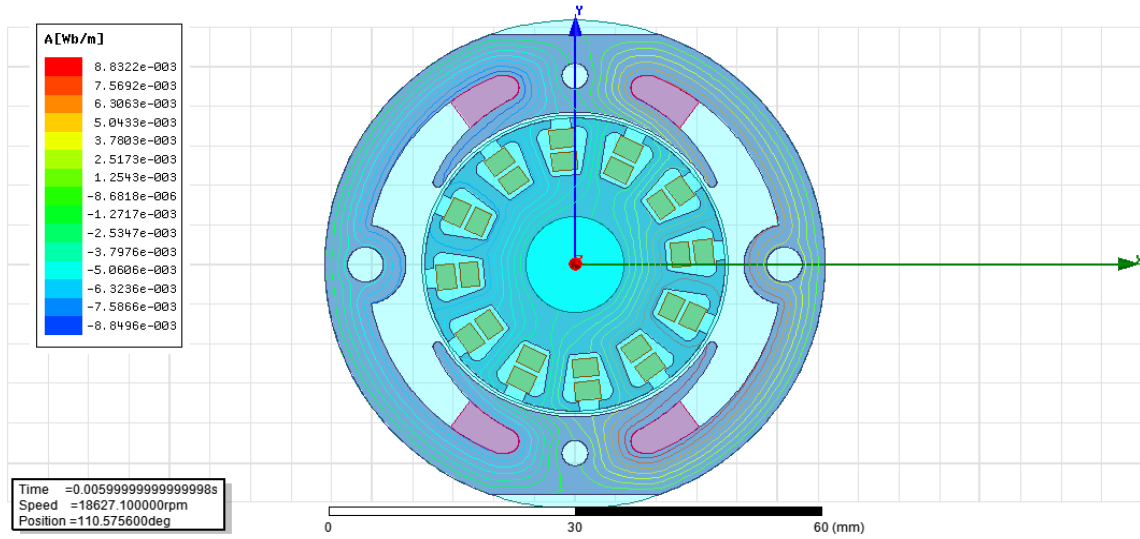


Figure 15. Magnetic flux lines of the motor

Fast fourier transform (FFT) of the model analyses is also carried out to know the harmonic with noise contained. To know the harmonic contained in torque and in winding current, its FFT analysis is given in Figure 16 and Figure 17. It shows the noise contains in torque and winding current.

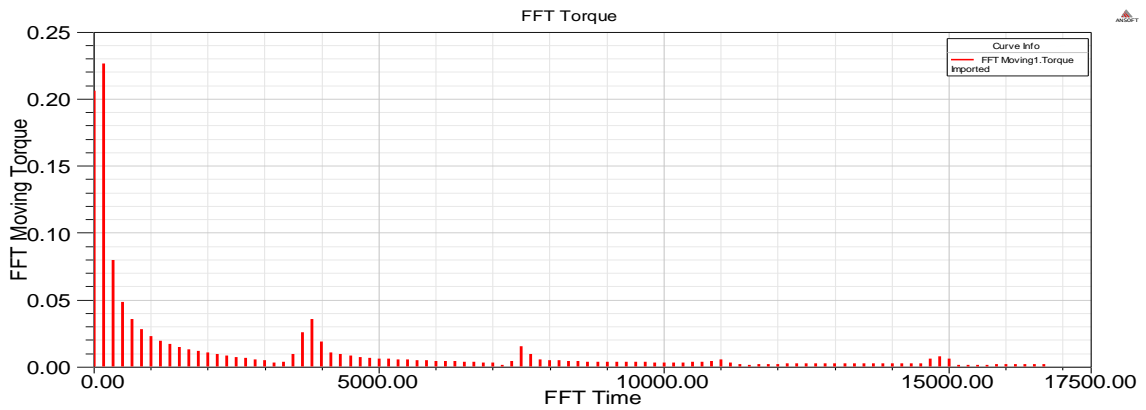


Figure 16. FFT graph of moving torque with the variation of time of the motor

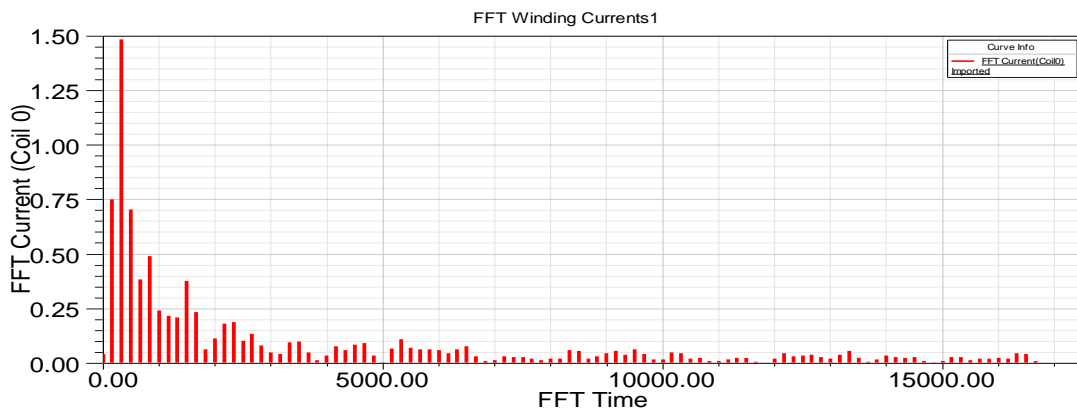


Figure 17. FFT graph of current with the variation time of the motor

#### 4. CONCLUSION

In this research paper, the universal motor is analysed with the help of the finite element method for agro applications. The motor performance was analysed with the variation of brush angle and pole embrace factor value. The optimum value of the variable is selected, and it observes that the model's efficiency is higher than the generalised motor. The efficiency of the optimal model at the optimum point of brush angle  $5^\circ$  and pole embrace value 0.65 is 73.15% and remain 26.85% will be the losses. This model is realised with good average torque as compared to the rest of the combinations of the variables. However, it also increases the current and speed of the motor. The rated torque and electromagnetic torque is enough to operate the motor for the proposed application. The flux density of the model is not saturated at the tooth of the universal motor. Further, the speed of the motor can be controlled with the speed control methods of the motor.




#### REFERENCES

- [1] R. Saidur, N. A. Rahim, M. R. Islam, and K. H. Solangi, "Environmental impact of wind energy," *Renew. Sustain. Energy Rev.*, vol. 15, no. 5, pp. 2423–2430, 2011, doi: 10.1016/j.rser.2011.02.024.
- [2] E. Taylor, "The Performance and Design of AC Commutator Motors: Including the Single-phase Induction Motors," *Wheeler Publishing*, Pitman: London, 1958.
- [3] G. Papa, B. K.-Seljak, B. Benedičič, and T. Kmecl, "Universal motor efficiency improvement using evolutionary optimization," *IEEE Trans. Ind. Electron.*, vol. 50, no. 3, pp. 602–611, 2003, doi: 10.1109/TIE.2003.812455.
- [4] P. Zásalický and J. Dupej, "Modeling of an Universal Motor Supplied by a Harmonic Voltage," *2006 12th International Power Electronics and Motion Control Conference*, 2006, pp. 1070–1073, doi: 10.1109/EPEPEMC.2006.4778543.
- [5] C. C. Chan and K. T. Chau, "Design of electrical machines by the finite element method using distributed computing," *Computers in Industry*, vol. 17, no. 4, pp. 367–374, 1991, doi: 10.1016/0166-3615(91)90049-F.
- [6] O. S. Daif, M. H. A. Raouf, M. A. Esmael, and A. E. B. Kotb, "Economic design of sleeve rotor induction motor using rotor ends," *International Journal of Electrical and Computer Engineering (IJECE)*, vol. 12, no. 2, pp. 1233–1242, 2022, doi: 10.11591/ijece.v12i2.pp1233-1242.
- [7] F. S. Ahmed, Z. S. Hussain, and T. K. M. Salih, "Enhancing performance for three-phase induction motor by changing the magnetic flux density and core material using COMSOL," *International Journal of Electrical and Computer Engineering (IJECE)*, vol. 12, no. 1, pp. 62–72, 2022, doi: 10.11591/ijece.v12i1.pp62-72.
- [8] K. Anumala and R. B. Veligatla, "Novel axial flux machines topology assessment and their feasible applications," *International Journal of Power Electronics and Drive Systems (IJPEDS)*, vol. 13, no. 1, pp. 84–92, 2022, doi: 10.11591/ijpeds.v13.i1.pp84-92.
- [9] M. F. M. Ab Halim, E. Sulaiman, M. Jenal, R. N. F. K. R. Othman, and S. M. N. S. Othman, "Preliminary analysis of eddy current and iron loss in magnetic gear in electric vehicle," *International Journal of Electrical and Computer Engineering (IJECE)*, vol. 12, no. 2, pp. 1161–1167, 2022, doi: 10.11591/ijece.v12i2.pp1161-1167.
- [10] D. S. Nayak and R. Shivarudraswamy, "Loss and Efficiency Analysis of BLDC Motor and Universal Motor by Mathematical Modelling in the Mixer Grinder," *Journal of The Institution of Engineers (India): Series B*, vol. 103, no. 2, pp. 517–523, 2022, doi: 10.1007/s40031-021-00652-z.
- [11] S. K. Sharma and M. S. Manna, "Performance Analysis of Universal Motor Based on Matlab Simulation," *2022 International Conference for Advancement in Technology (ICONAT)*, 2022, pp. 1–4, doi: 10.1109/ICONAT53423.2022.9726017.
- [12] Y. A. Yassin, A. N. Hussain, and N. Y. Ahmed, "Comparison and assessment of a different steel materials based on core losses reduction for three-phase induction motor," *International Journal of Power Electronics and Drive System (IJPEDS)*, vol. 12, no. 1, pp. 29–40, 2021, doi: 10.11591/ijpeds.v12.i1.pp29-40.
- [13] N. Abdullah, R. N. F. R. Othman, K. A. Karim, and L. S. Tat, "Analysis on EMF characteristics for torque ripple reduction in BLAC motor intended for HVLS fan application," *International Journal of Power Electronics and Drive System (IJPEDS)*, vol. 11, no. 4, pp. 2203–2211, 2020, doi: 10.11591/ijpeds.v11.i4.pp2203-2211.
- [14] T. C. Kwang, M. L. M. Jamil, and A. Jidin, "Improved magnetic behavior of hemicycle PM motor via stator modification," *International Journal of Electrical and Computer Engineering (IJECE)*, vol. 10, no. 3, pp. 3323–3332, 2020, doi: 10.11591/ijece.v10i3.pp3323-3332.
- [15] N. H. Quang, N. P. Quang, D. T. Hai, and N. N. Hien, "On tracking control problem for polysolenoid motor model predictive approach," *International Journal of Electrical and Computer Engineering (IJECE)*, vol. 10, no. 1, pp. 849–855, 2020, doi: 10.11591/ijece.v10i1.pp849-855.
- [16] A. L. Shuraiji, "The effect of static and dynamic eccentricities on the performance of flux reversal permanent magnet machine," *International Journal of Power Electronics and Drive System (IJPEDS)*, vol. 11, no. 2, pp. 634–640, 2020, doi: 10.11591/ijpeds.v11.i2.pp634-640.
- [17] H. Qi, L. Ling, C. Jichao, and X. Wei, "Design and research of deep slot universal motor for electric power tools," *Journal of Power Electronics*, vol. 20, no. 6, pp. 1604–1615, 2020, doi: 10.1007/s43236-020-00131-6.
- [18] D. R. Farrahov and A. K. Miniyarov, "Development of The Universal Apparatus for Induction Motors with Combined Winding Design," *2019 International Conference on Electrotechnical Complexes and Systems (ICOECS)*, 2019, pp. 1–4, doi: 10.1109/ICOECS46375.2019.8949978.
- [19] D. S. Nayak and R. Shivarudra Swamy, "Loss and Efficiency Analysis of Universal Motor Used in Mixer Grinder by Mathematical Modelling," *2018 IEEE International Conference on Automatic Control and Intelligent Systems (I2CACIS)*, 2018, pp. 105–110, doi: 10.1109/I2CACIS.2018.8603693.
- [20] K. Kurihara and S. Koseki, "New Design of High Output Equivalent 4-pole Universal Motor," *2018 XIII International Conference on Electrical Machines (ICEM)*, 2018, pp. 291–296, doi: 10.1109/ICELMACH.2018.8507152.
- [21] L. Xheladini, A. Tap, T. Aşan, M. Yılmaz and L. T. Ergene, "Permanent Magnet Synhronous Motor and Universal Motor comparison for washing machine application," *2017 11th IEEE International Conference on Compatibility, Power Electronics and Power Engineering (CPE-POWERENG)*, 2017, pp. 381–386, doi: 10.1109/CPE.2017.7915201.
- [22] A. Polat, L. T. Ergene and A. Firat, "Dynamic modeling of the universal motor used in washer," *International Aegean Conference on Electrical Machines and Power Electronics and Electromotion, Joint Conference*, 2011, pp. 444–448, doi: 10.1109/ACEMP.2011.6490640.




- [23] D. Lin, P. Zhou and S. Stanton, "An analytical model and parameter computation for universal motors," *2011 IEEE International Electric Machines & Drives Conference (IEMDC)*, 2011, pp. 119-124, doi: 10.1109/IEMDC.2011.5994773.
- [24] T. J. E. Miller and M. Willig, "Calculation of the armature inductance of the universal AC commutator motor," *The XIX International Conference on Electrical Machines - ICEM 2010*, 2010, pp. 1-6, doi: 10.1109/ICELMACH.2010.5607743.
- [25] Y. Niwa and Y. Akiyama, "The relation of a brush life to the commutator width and brush width ratio of a universal motor," *2009 International Conference on Power Electronics and Drive Systems (PEDS)*, 2009, pp. 1384-1389, doi: 10.1109/PEDS.2009.5385711.
- [26] K. Kurihara, K. Yamamoto and T. Kubota, "Commutation analysis of universal motors taking into account brush-to-bar voltage drop," *2009 International Conference on Electrical Machines and Systems*, 2009, pp. 1-4, doi: 10.1109/ICEMS.2009.5382653.
- [27] A. Di Gerlando and R. Perini, "Model of the commutation phenomena in a universal motor," *IEEE International Electric Machines and Drives Conference, 2003. IEMDC'03.*, 2003, pp. 173-179 vol.1, doi: 10.1109/IEMDC.2003.1211259.
- [28] D. M. Ionel, M. Popescu, S. J. Dellinger, T. J. E. Miller, R. J. Heideman and M. I. McGilp, "On the variation with flux and frequency of the core loss coefficients in electrical machines," in *IEEE Transactions on Industry Applications*, vol. 42, no. 3, pp. 658-667, May-June 2006, doi: 10.1109/TIA.2006.872941.
- [29] Rupam and S. Marwaha, "Mitigation of Cogging Torque for the Optimal Design of BLDC Motor," *2021 IEEE 2nd International Conference On Electrical Power and Energy Systems (ICEPES)*, 2021, pp. 1-5, doi: 10.1109/ICEPES52894.2021.9699544.
- [30] M. S. Manna, S. Marwaha, and N. Garg, "Modeling and Simulation of Linear Induction Motor By Using 2D Fem," *International Conf. On Power Systems Operations and Control*, 2010.
- [31] M. S. Manna, S. Marwaha, and H. M. Rai, "Application of a finite Element Method to find the Efficiency of Linear Induction Motor with Constant Voltage feeding," *International Journal of Electronics Engineering*, vol. 1, no. 1, pp. 41-43, 2009.
- [32] M. M. Tezcan, A. I. Çanakoğlu, A. G. Yetgin, A. Gün, B. Cevher and M. Turan, "Analysis of one phase special electrical machines using finite element method," *2017 International Conference on Electromechanical and Power Systems (SIELMEN)*, 2017, pp. 113-118, doi: 10.1109/SIELMEN.2017.8123321.
- [33] O. C. Zienkiewicz, R. L. Taylor, and J. Z. Zhu, "The finite element method: its basis and fundamentals," *Elsevier*, 2005.
- [34] ANSYS, "Maxwell Online Help, Version 14," vol. 15317, no. December, pp. 724-746, 2010.

## BIOGRAPHIES OF AUTHORS



**Sudhir Kumar Sharma**    received his B. Tech degree in electrical engineering from Rajasthan Technical University, Kota, India in 2015 and M. Tech degree in electrical engineering from Punjab Engineering College, Chandigarh, India in 2019. Currently, he is pursuing Ph.D. degree in electrical and instrumentation engineering from Sant Longowal Institute of Engineering and Technology, Punjab, India. His current research area of interest is electrical machine, power electronics, electric vehicles application, power system, and renewable sources. He can be contacted at email: sudhirs390@gmail.com.



**Manpreet Singh Manna**    is an Associate Professor at the Department of Electrical and Instrumentation Engineering, Sant Longowal Institute of Engineering and Technology, Punjab, India, where he has been a faculty member since 1997. He was former Director at AICTE, New Delhi, India, from 2014 to 2018. He received the B.E. degree in Electrical & Electronics Engineering from P.E.S. College of Engineering, Mandya, Karnataka, India in 1993, M.E. degree in Power and Machines from Thapar Institute of Engineering and Technology, Patiala, India in 2000, and Ph.D. degree in Electrical and Instrumentation Engineering from SLIET Longowal, Punjab, India in 2014. His research area of interest is power system, machine design, renewable sources, and electric vehicles application. He can be contacted at email: msmanna@ieee.org.